Progress In Electromagnetics Research, Vol. 118, 17–35, 2011

MULTIFOLDED BANDWIDTH BANCH LINE COUPLER WITH FILTERING CHARACTERISTIC USING COUPLED PORT FEEDING

Y. S. Wong*, S. Y. Zheng, and W. S. Chan

Department of Electronic Engineering, City University of Hong Kong, 83 Tat Chee Avenue, Kowloon, Hong Kong, China

Abstract—A new uni-planar structure branch-line coupler with broad bandpass response is proposed. Single section branch line couplers (SSBC) are popular due to their simplicity and ease of use but suffer from narrow return loss bandwidth and poor out of band rejection characteristics. The work presented here overcomes these limitations with the use of coupled port feeding. Through the study of input impedance of feeding network and single section branch line coupler, the bandwidth of the new coupler increased by almost 6-times. In addition, the coupler exhibited band-pass filtering characteristics. Measured results exhibited low insertion loss ($\leq$ 4-dB), small magnitude difference ($\leq$ 1-dB), good return loss and isolation ($\geq$ 10-dB) and small phase variation ($90^\circ \pm 5$) within the passband. A measured bandwidth of 58% was achieved with this single section coupled port fed branch line coupler at a centre frequency of 1-GHz. Its two output ports achieved rejection levels better than 25 dB in the stopband.

1. INTRODUCTION

Hybrid couplers and filters are the most common components found in wireless communication systems. However, the popular realization using microstrip in the form of a branch line coupler is only suitable for applications with narrow bandwidth. Although it has narrow bandwidth, its out of band characteristics have insufficient selectivity for adequate performance as a filter. A cascade connection of couplers with filter is the common solution [1], however this results in larger size. The resulting cascade also invariably degrades each

Received 14 April 2011, Accepted 30 May 2011, Scheduled 20 June 2011

* Corresponding author: Yuk Shing Wong (markwong0909@gmail.com).

individual components performance as they are normally designed and optimized separately. Wideband couplers have been proposed with excellent performance, at the expense of size [2, 3], high characteristic impedances which result in narrow line widths [3, 4], multi-layer technology [5] and poor return loss ($< 10\,\mathrm{dB}$) in the passband [6]. Couplers with harmonic suppression have also been proposed, with most resonant elements providing suppression to harmonics only [7–9]. Lumped element [10, 11] techniques do not suffer from such resonance effect however they do suffer from tolerance problems and tend to have a high insertion loss.

Coupled lines are a common realization of microwave filters. However, Sun and Zhu [12] reported several drawbacks including narrow passband bandwidth, tight coupling, high insertion loss, limited stopband and lower Q-factor. Some research works have been done to extend the stopband but invariably results in narrower passband bandwidth [13–15]. The multi-mode resonators [12] is an approach used to increase bandwidth to more than 100%, however it cannot improve the bandwidth of the other interconnected components.

Circuit integration is a straightforward approach in resolving the above problems with the concept already demonstrated with balun filters [16–20] which combine out of phase power division with band-pass filtering function. The coupler filter proposed by Uysal and Watkins [21, 22], made by non-uniform transmission lines had a relative bandwidth of 18% but occupied an area of more than 2-wavelengths by 5-wavelengths at the center frequency. Therefore, small size and wide bandwidth are found in antenna and feeding network integration [23]. However, [23] has no compatibilities of other components and design criteria. The use of port extension is a way of improving existing components, such as for the dual-band coupler [24] and dual-band power divider [25]. Series stubs when used as matching network [26] for branch line hybrid couplers doubled its original bandwidth. A multi-folded increase in bandwidth by feeding each port using coupled lines resulting in filter type response for branch line couplers has never been proposed.

In this paper, two single section branch line couplers (SSBC) with coupled port feeding are introduced and analyzed with the aim of achieving the following characteristics.

1. Wideband
2. Low insertion loss (better than $4\,\mathrm{dB}$)
3. Small amplitude imbalance ($1\,\mathrm{dB}$)
4. Small phase variation ($90^\circ \pm 5^\circ$)
5. Single layer planar structure

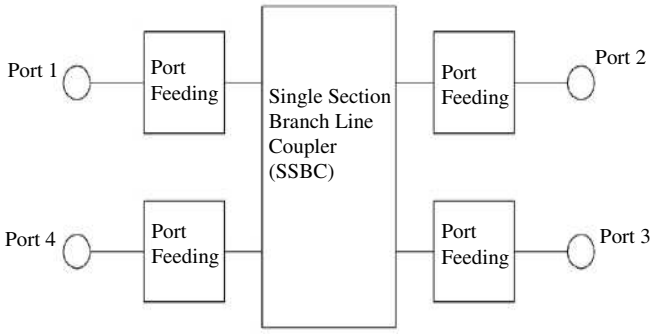

Figure 1. The analysis model.

6. Bandpass response

This work begins in Section 2, where the single section branch line coupler (SSBC) with the three different port feeding networks are theoretically analyzed and compared. Fig. 1 shows the proposed circuit model, all the ports of single section branch line coupler are connected to the feeding network. The comparison focuses on the principle behind how improvement is achieved with this feeding network. Experimental results for these couplers are given and discussed in Section 3. Finally, this paper is concluded in Section 4.

2. THEORETICAL ANALYSIS

The analysis focuses on the port feeding network which forms the basis of improvement in performance that includes passband bandwidth and stopband suppression level. For ease of analysis the even and odd modes of the coupled lines structure are assumed to have the same propagation velocity.

2.1. Conventional Branch Line Coupler without extra Feeding Network

Figure 2(a) shows the conventional branch line coupler constructed using 2 pairs of quarter wavelength transmission lines and is symmetrical across two central planes. The signal is fed directly to the coupler without extra feeding network. In the analysis, the coupler is reduced to four 1-port networks [24] which are shown in Fig. 2(b). The S parameters are a function of the four modes reflection coefficient (Γ_{mq}) and their relationship are shown in (1)–(4). According

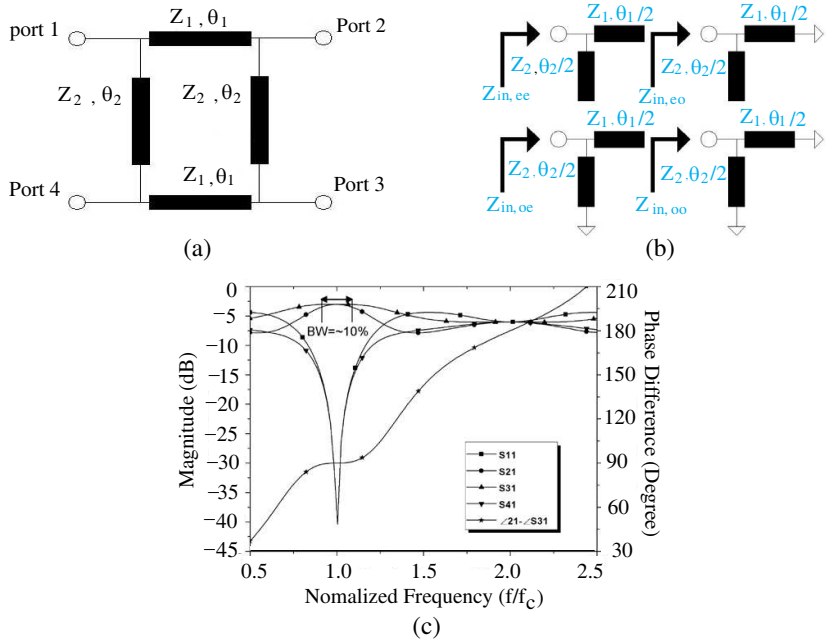

Figure 2. Conventional branch line coupler. (a) Transmission line model, (b) analysis model of 1-port networks in 4 different modes, (c) theoretical S-parameter.

to Fig. 2(b), the input impedance ($Z_{in,mq}$) of each mode is simple to determine and its corresponding reflection coefficient is found by (5). In calculating input impedance (6)–(10), v is defined as the frequency difference between centre frequency (f_c) and measurement frequency (f), and in more detail the mathematical definition is shown in (11)–(13). Using this definition simplifies the design of the coupler filter for a required bandwidth and is easy to observe its maximum bandwidth. Using (1)–(13), the S parameters of the SSBC can be calculated. Fig. 2(c) shows the theoretical response of this ideal branch line coupler. Its bandwidth can be seen to be narrow and without harmonic suppression.

$$S_{11} = S_{22} = S_{33} = S_{44} = \frac{\Gamma_{ee} + \Gamma_{eo} + \Gamma_{oe} + \Gamma_{oo}}{4} \tag{1}$$

$$S_{21} = S_{12} = S_{43} = S_{34} = \frac{\Gamma_{ee} - \Gamma_{eo} + \Gamma_{oe} - \Gamma_{oo}}{4} \tag{2}$$

$$S_{31} = S_{42} = S_{13} = S_{24} = \frac{\Gamma_{ee} - \Gamma_{eo} - \Gamma_{oe} + \Gamma_{oo}}{4} \tag{3}$$

$$S_{41} = S_{32}S_{23} = S_{14} = \frac{\Gamma_{ee} + \Gamma_{eo} - \Gamma_{oe} - \Gamma_{oo}}{4} \tag{4}$$

$$\Gamma_{mq} = \frac{Z_{in,mq} - 1}{Z_{in,mq} + 1} \tag{5}$$

$$Z_{in,mq} = Z_{1,m}//Z_{2,q}, \quad m = e, o;\ q = e, o \tag{6}$$

$$Z_{in,ee} = \frac{-jZ_1Z_2}{v(Z_1 + Z_2)} \tag{7}$$

$$Z_{in,eo} = \frac{-jZ_1Z_2v}{Z_1k^2 - Z_2} \tag{8}$$

$$Z_{in,oe} = \frac{jZ_1Z_2v}{Z_1 - Z_2v^2} \tag{9}$$

$$Z_{in,oo} = \frac{jZ_1Z_2v}{Z_1 + Z_2} \tag{10}$$

$$v = \frac{1 - \tan\Delta\vartheta}{1 + \tan\Delta\vartheta} \tag{11}$$

$$\Delta\vartheta = \left(\frac{1 + \Delta f}{2}\right)\left(\frac{\pi}{2}\right) \tag{12}$$

$$\Delta f = f_c \pm f \tag{13}$$

2.2. Quarter-wavelength Port Feeding Network

Directly connecting quarter-wavelength transmission line feeding network to all four ports of the SSBC is a method that can be used to increase its bandwidth. Fig. 3 shows the transmission line model of the branch line coupler with quarter-wavelength feeding networks. (14) shows the ABCD matrix of the quarter-wavelength transmission line network, where Z_T and θ_T are the characteristic impedance and electrical length respectively of the feeding network. This matrix is used to obtain the theoretical response.

$$[FN] = \begin{bmatrix} \cos\theta & jZ_T\sin\theta \\ jY_T\sin\theta & \cos\theta \end{bmatrix}; \quad Y_T = 1/Z_T \tag{14}$$

The $\lambda/4$ feeding network is simple and easy to design using computer-aided tool. However, even for a two section feeding network, the theoretically calculated maximum bandwidth is only around 30% [27]. This is at the expense of a five-fold increase in size, and it still cannot filter out-of-band signals. The design method [27] is complex and not general enough for most applications for a wideband coupler. Here the design equations are re-organized; these equations could be applied to other feeding network for branch line couplers.

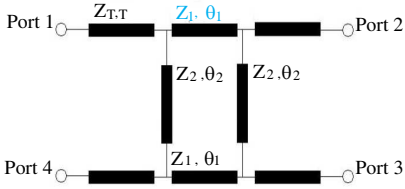

Figure 3. The branch-line coupler with $\lambda/4$ feeding network.

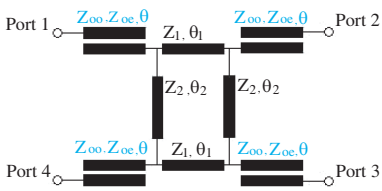

Figure 4. The branch-line coupler with symmetrical coupled lines as port feeding network.

A coupler is designed for equal power division with quadrature phase difference good return loss and isolation; the relationship between the four mode reflection coefficients is summarized in (15).

$$\Gamma_{ee} = j\Gamma_{oo} = -\Gamma_{eo} = -j\Gamma_{oe} \tag{15}$$

$$\Gamma_{mq} = \frac{\left(jZ_T^2k + Z_TZ_{in,mq}\right) - \left(Z_T + jkZ_{in,mq}\right)}{\left(jZ_T^2k + Z_TZ_{in,mq}\right) - \left(Z_T + jkZ_{in,mq}\right)},\ m = e,o;q = e,o; \tag{16}$$

The central part of the coupler is the ideal classic branch line coupler, $Z_1 = 41\,\Omega$ and $Z_2 = 59.5\,\Omega$ are chosen in [3] for the best minimum amplitude imbalance bandwidth. Its performance is primarily determined by the characteristic impedance of the $\lambda/4$ feeding network. Using (7)–(10) and (16), each mode reflection coefficient after the feeding network can be calculated. There is a correlation between characteristic impedance of feeding network, bandwidth and bandwidth definition Since k is a function of bandwidth (17), (18), (20)–(22) are the relationship between bandwidth and characteristic impedance of the feeding network. In general, the return loss at the centre frequency is reduced the most, and at centre frequency can be found by (19).

$$\frac{kZ_T + c}{k^2Z_T^2 + Z_Tc} = \frac{kZ_T^2 - Z_T(ck+1) + k^2c}{kZ_T^2 - Z_T(ck-1) - k^2c} \tag{17}$$

$$c = \frac{1}{1+\sqrt{2}} \tag{18}$$

$$S_{11} = \frac{j\sqrt{8}Z_T^2\left(Z_T^4+1\right)}{4Z_T^4 + \left(Z_T^4+1\right)^2};\quad Z_T \neq 1 \tag{19}$$

$$k = \frac{1-\tan\Delta\vartheta}{1+\tan\Delta\vartheta} \tag{20}$$

$$\Delta\vartheta = \left(\frac{1+\Delta f}{2}\right)\left(\frac{\pi}{2}\right) \tag{21}$$

$$\Delta f = \mathrm{BW}/2 \tag{22}$$

2.3. Symmetrically Coupled Port Feeding Network

In the previous section, the use of $\lambda/4$ feeding network was analyzed theoretically. It was found to improve the bandwidth but was very limited especially with the large increase in circuit size and poor ability in separating two reflection zeros. To significantly improve the bandwidth without significantly increasing the circuit size, symmetrically coupled lines are considered next. With the use of coupled lines, additional function can also be considered due to its inherent resonator type characteristic. This integration of multi-function within the same component can be considered as another form of circuit minimization. It was found to provide more degrees of freedom in coupling coefficient and impedance over a wider frequency range.

The transmission line model of these coupled lines connected to all four ports of the SSBC is shown in Fig. 4. These coupled lines form the core of port connection as well as impedance transformation and filter simultaneously, which is used to suppress out-of-band signals. Suppression in the lower band is due to the inherent nature of the frequency dependent coupled lines through impedance mismatch due to decreased coupling (23), (24).

$$Z^e_{in,mq} = Z_{oe}\frac{Z_{in,mq} + jZ_{oe}\tan\theta}{Z_{oe} + jZ_{in,mq}\tan\theta}; \quad Z_{oe} = \sqrt{\frac{1+C}{1-C}} \tag{23}$$

$$Z^o_{in,mq} = Z_{oo}\frac{Z_{in,mq} + jZ_{oo}\tan\theta}{Z_{oo} + jZ_{in,mq}\tan\theta}; \quad Z_{oo} = \sqrt{\frac{1-C}{1+C}} \tag{24}$$

where C is the coupling coefficient of the coupled lines and the coupled lines structure are assumed to have the same even and odd mode propagation velocity ($\theta = \theta_e = \theta_o$).

Even order harmonics are naturally rejected by the coupled lines, and its transmission zero can be found in Equation (29). S_{21} is equal to zero when C_a is zero. C_a is also zero when the operating frequency is 2 times the centre frequency (f_c), due to the coupled lines being quarter-wavelength at the centre frequency. Therefore, impedance transformation and filtering can be implemented simultaneously using coupled lines connected to the four ports. Coupled lines are analyzed using even and odd mode analysis represented by a two port ABCD

matrix [28], the matrix elements are shown in (25)–(29).

$$[FN] = \begin{bmatrix} A_s & B_s \\ C_s & D_s \end{bmatrix} \tag{25}$$

$$A_s = D_s = \frac{Z_{oe}\cot\theta + Z_{oo}\cot\theta}{Z_{oe}\csc\theta - Z_{oo}\csc\theta} \tag{26}$$

$$B_s = \frac{j}{2}\left[\frac{Z_{oe}^2 + Z_{oo}^2 - 2Z_{oe}Z_{oo}\left(\cot^2\theta + \csc^2\theta\right)}{Z_{oe}\csc\theta - Z_{oo}\csc\theta}\right] \tag{27}$$

$$C_s = \frac{2j}{Z_{oe}\csc\theta - Z_{oo}\csc\theta} \tag{28}$$

$$S_{21}_{f=2f_c} = \frac{2C_aZ_0}{A_aC_aZ_0 + A_aD_a - 1 + (C_aZ_0)^2 + D_aC_aZ_0} \tag{29}$$

where $C_a = 0$; $A_a \neq 0$; $D_a \neq 0$.
$f=2f_c$ $f=2f_c$ $f=2f_c$

In Fig. 5(a), two transmission zeros can be seen, (25)–(29) with the upper transmission zero found to be 2 times that of the passband centre frequency. In Figs. 5(a) and 5(b), the bandwidth of the SSBC with symmetrically coupled lines is about 5 times that of the SSBC. Its bandwidth is also flatter than the one with quarter-wavelength port feeding networks. A SSBC design is based on four quarter-wave-length transmission lines to give perfect matching and quadrature power division, however this condition holds true only at centre frequency. Away from centre frequency, the input impedance (Z_{in}) deviates from the reference port impedance (Z_0) due to the change of electrical length away from a quarter wavelength. This mismatch at each port is further compounded by the other ports also being mismatched, resulting in an even narrower return loss bandwidth. As a result the coupler is not

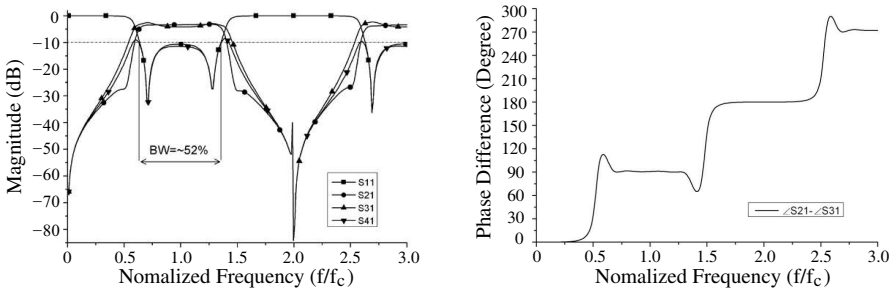

Figure 5. The response of the Branch line coupler with symmetrical coupled port feeding network.

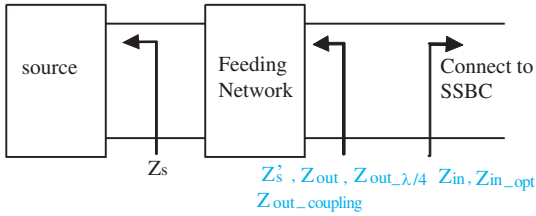

Figure 6. Analysis model for SSBC at each port.

able to operate over a wide bandwidth, and this effect can be seen in each mode analysis equation. In summary, the input impedance (Z_{in}) of the SSBC is correlated to the operating frequency (30) and each port termination. It is difficult to find a general solution analytically for the input impedance of the coupler, so the feeding network for the coupler is difficult to design. Under matched conditions as shown in Fig. 6, input impedance (Z_{in}) can be determined by (31). Using this method, suitable termination impedance (Z_{in_opt}*) for the SSBC can simply be determined from (30) and (31). Apart from good return loss, good isolation and quadrature power division are as important criteria in coupler design Suitable termination impedance can be found using (15). In the analysis, ideal lossless impedance transformers are placed at all ports of the coupler. The reference port impedance (Z_0, Z_s) is transformed to the impedance ($Z'_s = Z_{in\_opt}$*), giving equal power division with quadrature phase difference at that particular frequency point. The results (Z_{in_opt}*) from the analysis are shown in Figs. 7(a) and (b).

$$Z_{in,1} = F(f, Z_{in,q}); \quad q = 2, 3, 4 \tag{30}$$

where $Z_{in,q}$ is the terminated impedance in each port,

$$Z_{in\_opt}* = Z'_s = Z_{out} \tag{31}$$

Since one port of the feeding network in Fig. 6 is terminated by reference impedance (Z_0) the output impedance of ($Z_{out\_\lambda/4}$) and ($Z_{out\_coupling}$) are simply found by substituting (14) and (25) into (23), (24). The computed results are shown in Figs. 7(a) and (b). Comparing 3 impedance lines in Fig. 7(b), it can be seen that the output impedance ($Z_{out\_\lambda/4}$) only matches the imaginary part of the ideal impedance (Z_{in_opt}*) around the centre frequency. In Fig. 7(a), the reference port impedance is decreased by the transformer even at the centre frequency, which leads to poor return loss (S_{11}) at the centre frequency. The nonlinear change of the SSBC input impedance (Z_{in_opt}) makes the low order feeding network difficult to realize the required impedance, resulting in insignificant improvement. However,

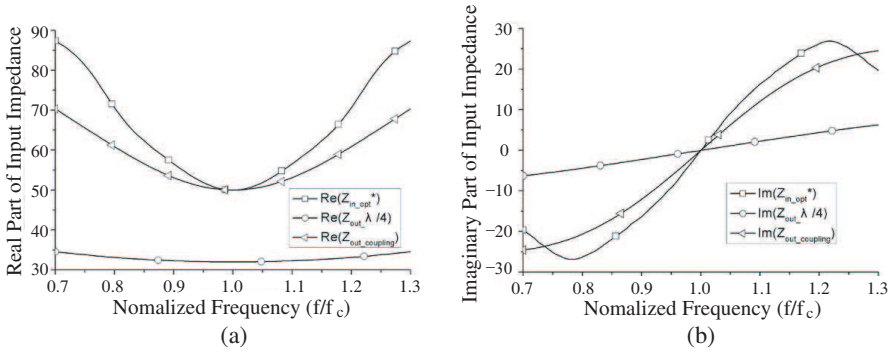

Figure 7. (a) Real part of input impedance, (b) imaginary of the input impedance.

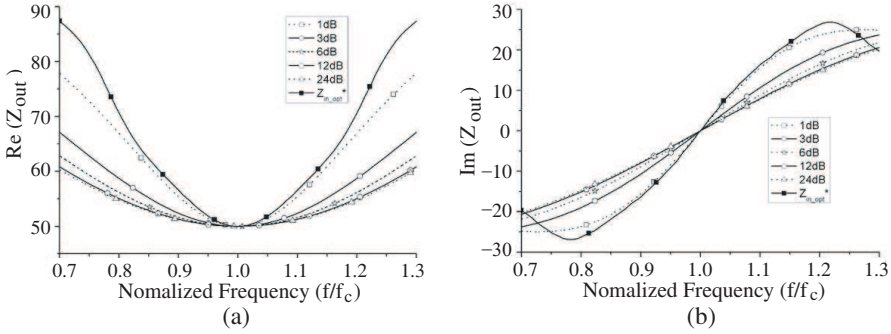

Figure 8. The relationship between coupling coefficient and input impedance. (a) Real part of the input impedance, (b) imaginary part of the input impedance.

the coupled line output impedance ($Z_{out\_coupling}$) exhibits a non-linear change with frequency. Using this non-linear characteristic, an overall flat response can be obtained. And a good return loss is expected in the passband.

Figures 8(a) and (b) show the reference port impedance transformed by the symmetrical coupled lines for different coupling coefficients. The change of output impedance ($Z_{out\_coupling}$) is mainly determined by the coupling coefficient of the symmetrical coupled lines. The tighter coupling coefficient makes the output impedance ($Z_{out\_coupling}$) closer to the ideal impedance (Z_{in_opt}*), resulting in a better response but with narrower bandwidth. The weaker coupling coefficient results in broader bandwidth but with poorer passband response.

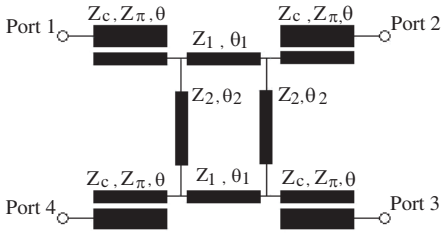

Figure 9. The schematic of the coupler using asymmetrical coupled port feeding network.

2.4. Asymmetrically Coupled Port Feeding Network

In Section 2.3, the branch-line coupler exhibits a flat bandpass response with the use of symmetrically coupled feeding networks connected to all input/output ports. Both line impedances are equal, which limits the design freedom. In addition, the practical coupling coefficient is limited and cannot be too large due to the constraint on narrow line width and small gap dimensions which makes fabrication difficult. The use of asymmetrically coupled lines is considered as an alternative to further increase the degree of freedom. Fig. 9 shows the schematics of the SSBC with asymmetric coupled port feeding network. The asymmetric coupled lines are analyzed using c and π modes analysis [29] as a 2-port ABCD matrix (32)–(36). R_c and R_π are the voltage ratio of the two lines, while Z_c and Z_π are the characteristic impedances of the two lines. Since the asymmetric coupled port feeding network is based on the principle behind quarter-wavelength impedance transformer by comparing this matrix with the result in Sections 2.2 and 2.3, the design equation of this asymmetrical coupled port feeding network can be found and are summarized in (37)–(40).

$$[IS] = \begin{bmatrix} A_a & B_a \\ C_a & D_a \end{bmatrix} \tag{32}$$

$$A_a = \frac{R_c^2 Z_{c1}\left(1-\frac{R_\pi}{R_c}\right)\cot\theta_c + R_\pi^2 Z_{\pi 1}\left(1-\frac{R_c}{R_\pi}\right)\cot\theta_\pi}{R_c^2 Z_{c1}\left(1-\frac{R_\pi}{R_c}\right)\csc\theta_c + R_\pi Z_{\pi 1}\left(1-\frac{R_c}{R_\pi}\right)\csc\theta_\pi} \tag{33}$$

$$B_a = \frac{A_a D_a - 1}{C_a} \tag{34}$$

$$C_a = \frac{j\left(1-\frac{R_c}{R_\pi}\right)\left(1-\frac{R_\pi}{R_c}\right)}{R_c Z_{c1}\left(1-\frac{R_\pi}{R_c}\right)\csc\theta_c + R_\pi Z_{\pi 1}\left(1-\frac{R_c}{R_\pi}\right)\csc\theta_\pi} \tag{35}$$

$$D_a = \frac{Z_{c1}\left(1-\frac{R_\pi}{R_c}\right)\cot\theta_c + Z_{\pi 1}\left(1-\frac{R_c}{R_\pi}\right)\cot\theta_\pi}{R_c Z_{c1}\left(1-\frac{R_\pi}{R_c}\right)\csc\theta_c - R_\pi Z_{\pi 1}\csc\theta_\pi} \tag{36}$$

$$\frac{Z_{c2}}{Z_{c1}} = \frac{Z_{\pi 2}}{Z_{\pi 1}} = -R_c R_\pi \tag{37}$$

$$\frac{Z_{\pi 1}}{Z_{c1}} = \frac{R_\pi}{R_c} \tag{38}$$

$$Z_\pi = 2Z_T - Z_c \tag{39}$$

$$Z_c = Z_T \pm \sqrt{Z_T^2 - \left(4Z_T^2 + {}^1\!/_2\right)} \tag{40}$$

Using (17), Z_T is defined by the separation of two reflection zeros. Using Z_T to solve (37)–(40) simultaneously, the S-parameters are obtained and shown in Fig. 10.

Since relative bandwidth is correlated to the core component, the SSBC with different port feeding are summarized and compared and shown in Table 1. The bandwidth of the classic SSBC ($\mathrm{BW_{SSBC}}$ =10%) is used as a reference for ease of comparison.

In Table 1, the bandwidths of the SSBC can be observed to have significant improvement using both symmetric coupled feeding network (SCFN) and asymmetric coupled feeding network (ACFN). For maximum bandwidth, the coupler using ACFN has the most significant bandwidth improvement compared with other feeding networks which occupies equal size. When considering size, the coupler using series stub, SCFN and ACFN are similar, but are smaller than the double $\lambda/4$ feeding network and T shape feeding network. The series stub in Ref. [26] realized using interdigital coupled lines has a bandwidth improvement of two-times. The improvement is smaller than that for the edge coupled lines. For the interdigital case, it has a similar layout to the edge coupled line but it would be contradictory if these two ABCD matrices are set equal. B_s and B_a for the edge coupled

Table 1. SSBC with different feeding network (*FN*).

Feeding Network (*FN*)	Bandwidth	Size
Double $\lambda/4$ FN in Ref. [27]	$3 \times \mathrm{BW_{SSBC}}$	$0.25\lambda_\mathrm{c} \times 1.25\lambda_\mathrm{c}$
T shape *FN* in Ref. [2]	$4 \times \mathrm{BW_{SSBC}}$	$0.25\lambda_\mathrm{c} \times \lambda_\mathrm{c}$
Series stub in Ref. [26]	$3 \times \mathrm{BW_{SSBC}}$	$0.25\lambda_\mathrm{c} \times 0.75\lambda_\mathrm{c}$
SCFN in Section 2.3	$52 \times \mathrm{BW_{SSBC}}$	$0.25\lambda_\mathrm{c} \times 0.75\lambda_\mathrm{c}$
ACFN in Section 2.4	$58 \times \mathrm{BW_{SSBC}}$	$0.25\lambda_\mathrm{c} \times 0.75\lambda_\mathrm{c}$

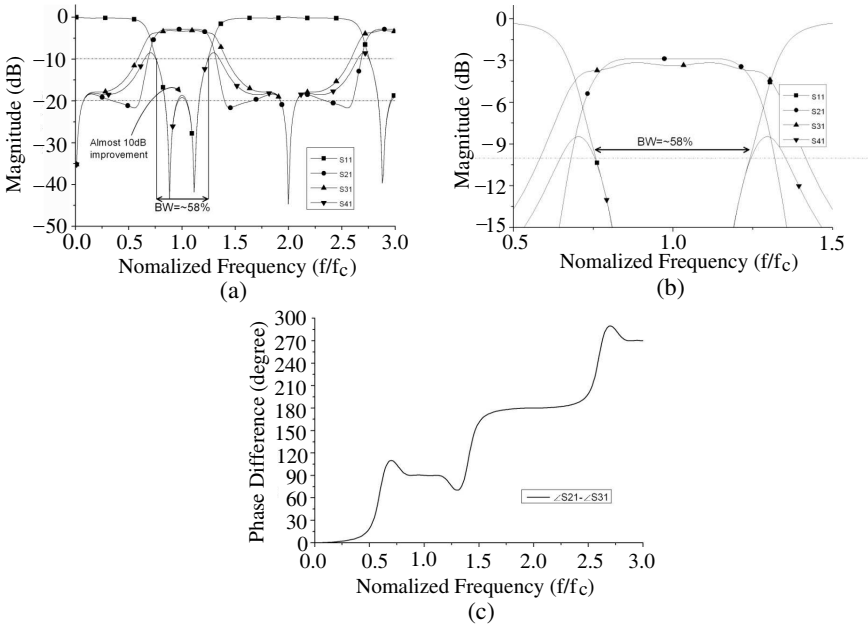

Figure 10. The theoretical response of asymmetrically coupled port feeding network.

lines are purely imaginary, since the impedance cannot be complex. B_i for the series stub is a complex number with non-zero real parts which leads to significantly different characteristics. The resulting difference in bandwidth demonstrates the difference between the two coupling methodologies. Fig. 11(a) shows the attenuation of the two networks, although the interdigital coupled lines has a notched response around the second harmonic, the transition band for the interdigital case in [26] is much wider than the transition band of edge coupled lines. Apart from the stopband response, the different characteristic can also be observed from the passband VSWR. The U-shape VSWR implies that the edge coupled network has a bandpass response, but this is not present for interdigital coupled lines in [26].

Refs. [1] and [22] are the few reported quadrature coupler with filtering characteristic, and their performances are shown and compared in Table 2. In comparison, Ref. [22] has the largest physical size, while Ref. [1] is the second largest. Couplers with SCFN and ACFN are equal in size, which are 40-times smaller than in Ref. [1] and 77-times smaller than in Ref. [22]. In Ref. [22], only one port has bandpass characteristic, resulting in few practical applications. Also the maximum bandwidth is a major concern in coupler design with

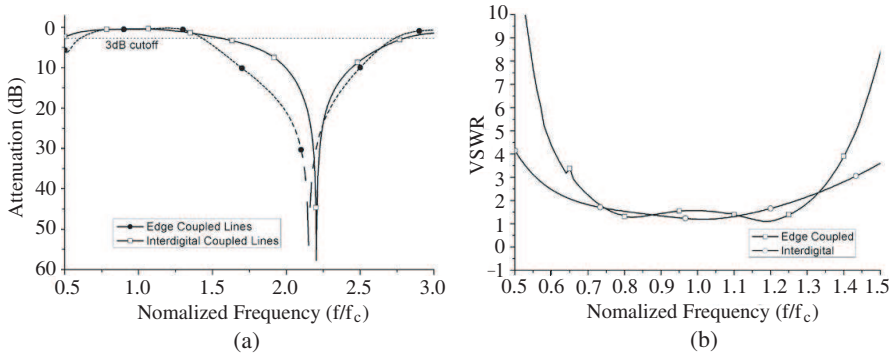

Figure 11. (a) Attenuation, (b) passband VSWR.

the 18% measured bandwidth in Ref. [22] being defined by a coupling factor of 4.1 ± 0.25 dB. The measured bandwidth in Ref. [1] is 10% with defined with a coupling factor of 5 ± 0.3 dB. The coupler with SCFN and ACFN has more than 50% bandwidth with a coupling factor of 3.4 ± 0.6 dB. In summary, the coupler with ACFN has the flattest and widest coupling response (-3 dB) and with the smallest size.

3. EXPERIMENTAL RESULTS

In this section, verification of the proposed coupler filter configuration is performed using a design example operating at a centre frequency of 1 GHz. The coupler filter was realized using Roger Duriod 5870 with $\varepsilon_r = 2.33$, $h = 1.575$ mm.

Using simulation software Ansoft HFSS, the SSBC with asymmetrically coupled feeding network is designed for maximum bandwidth taking into account the effects of junction discontinuities. However, the T-junction discontinuities result in a minimal parasitic resonance within the stopband which cannot be avoided. The resulting characteristic impedances are $Z_1 = 40\,\Omega$, $Z_2 = 59\,\Omega$; while all the

Table 2. Coupler with bandpass response.

Type of Coupler Filter	Bandwidth	Size
Connection in Ref. [1]	10%	$1.58\lambda_c \times 4.74\lambda_c$
Coupler filter in Ref. [22]	18%	$2.69\lambda_c \times 5.39\lambda_c$
Coupler using SCFN	52%	$0.25\lambda_c \times 0.75\lambda_c$
Coupler using ACFN	58%	$0.25\lambda_c \times 0.75\lambda_c$

Table 3. The physical dimension of the coupler with asymmetrically coupled port feeding network.

	Corresponded Value
W_1	6.5 mm
L_1	47.8 mm
W_2	3.4 mm
L_2	50.3 mm
INW	1.6 mm
INW_1	0.5 mm
INL	52 mm
GAP	0.3 mm
$Offset$	0.23 mm

lines remain at quarter-wavelength ($\theta = \theta_1 = \theta_2 = 90°$) long. The corresponding physical dimensions of the final coupler are summarized in Table 3. Its layout is shown in Fig. 12, where the hatched areas are the transmission lines of the coupler. The centeral SSBC are connected to 4 pairs of asymmetric coupled lines. A picture of the SSBC with asymmetric port feeding networks is shown in Fig. 13, with an enlarged view of the asymmetric lines shown in the upper right hand corner.

From the results shown in Fig. 14, the measured results follow closely to simulation. The simulated S-parameters at 1 GHz are: $S_{11} = -25.2$ dB, $S_{21} = -2.9$ dB, $S_{31} = -3.8$ dB, $S_{41} = -22.8$ dB, $(\angle S_{21} - \angle S_{31}) = 90.5°$. While the measured S-parameters at 1 GHz are: $S_{11} = -28.9$ dB, $S_{21} = -2.9$ dB, $S_{31} = -3.9$ dB, $S_{41} = -29.9$ dB, $(\angle S_{21} - \angle S_{31}) = 88.3°$. The bandwidth is defined here using amplitude imbalance within the passband to be smaller than 1 dB with Return loss (S_{11}) and isolation (S_{41}) below -10 dB. S_{21} and S_{31} are above -4 dB with a low loss and a phase difference within $90 \pm 5°$. The

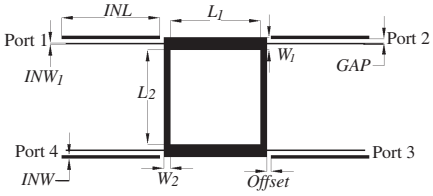

Figure 12. The layout of the coupler with ACFN.

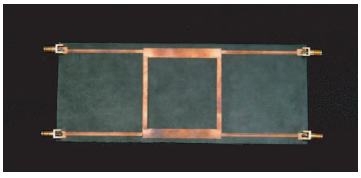

Figure 13. The top view of the fabricated coupler using ACFN.

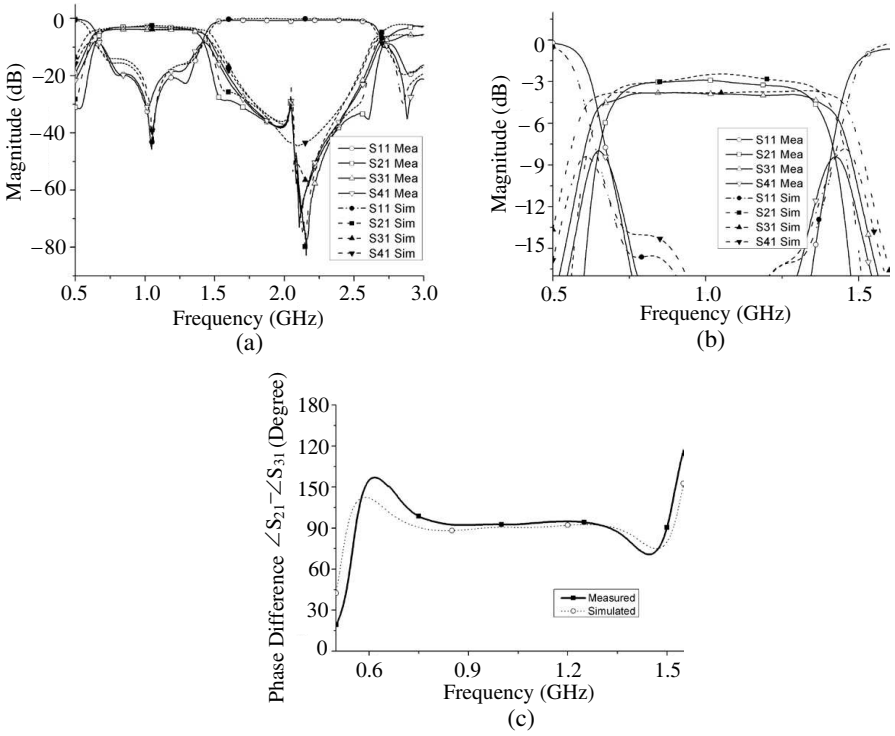

Figure 14. The simulated result and the measured result of the coupler with the proposed feeding network.

predicted bandwidth is 65% at a centre frequency of 1 GHz, while the measured bandwidth is 58% at a centre frequency of 1.03 GHz. In the theoretical analysis, the transmission zero for S_{21} and S_{31} is 2 GHz ($2f_o$); the transmission zeros after junction compensation shift to 2.15 GHz with -79 dB for Port 2 (S_{21}), 2.17 GHz with a values of -56 dB for Port 3 (S_{31}). Measured transmission zero for Port 2 is 2.11 GHz and for Port 3 is 2.15 GHz with -82 dB suppression which agrees well with simulation.

4. CONCLUSION

A wide passband quadrature coupler with bandpass response has been proposed and theoretically analyzed. It has been verified successfully through simulation and measurement. This new circuit is realized using a single section branch-line coupler with asymmetric port feeding networks, resulting in an extraordinarily wide bandwidth that also

has bandpass filtering characteristics. The relative bandwidth of the coupler was improved by 5.8 times compared with the original SSBC. Also, this coupler is much smaller than other previously reported wideband couplers with filters. The SSBC with the proposed asymmetrically coupled port feeding networks maintain a lower insertion loss than the individual but direct connection of coupler with filter. The proposed coupler exhibits low insertion loss, good return loss and good even order harmonic suppression, which agrees very well with the theoretical results. The proposed coupler filter will serve as a good candidate for wideband wireless communication application because of its multi-function characteristics, together with wide-band characteristics.

ACKNOWLEDGMENT

The work described in this paper was fully supported by the GRF grant from the Research Grants Council of the Hong Kong Special Administrative Region, China (Project No. 9041555).

REFERENCES

1. Sergio, L.-R., G.-L. Alejandro, S.-P. Magdalena, D.-E. Ana Isabel, G.-V. Juan Sebastian, and P.-C. Manuel Jesua, "Microstrip filter and power divider with improved out-of-band rejection for a Ku-band input multiplexer," *Microwave Conference, (EuMC)*, 315–318, Munich, Germany, Oct. 2003.
2. Riblet, G. P., "A directional coupler with very flat coupling," *IEEE Trans. Microw. Theory Tech.*, Vol. 26, No. 2, 70–74, Feb. 1978.
3. Muraguchi, M., T. Yukitake, and Y. Naito, "Optimum design of 3 dB branch-line couplers using microstrip lines," *IEEE Trans. Microw. Theory Tech.*, Vol. 31, No. 8, 674–678, Aug. 1983.
4. Chun, Y.-H. and J.-S. Hong, "Compact wide-band branch-line hybrids," *IEEE Trans. Microw. Theory Tech.*, Vol. 54, No. 2, 704–709, Feb. 2006.
5. Tang, C.-W., M.-G. Chen, Y.-S. Lin, and J.-W. Wu, "Broadband microstrip branch-line coupler with defected ground structure," *Electron. Lett.*, Vol. 42, No. 25, 1458–1460, Dec. 2006.
6. Paco, P. D., J. Verdu, O. Menendez, and E. Corrales, "Branch-line coupler based on edge-coupled parallel lines with improved balanced response," *IEEE Trans. Microw. Theory Tech.*, Vol. 56, No. 12, 2936–2941, Dec. 2008.

7. Kim, J.-S. and K.-B. Kong, "Compact branch-line coupler for harmonic suppression," *Progress In Electromagnetics Research C*, Vol. 16, 233–239, 2010.
8. Li, B., X. Wu, and W. Wu, "A miniaturized branch-line coupler with wideband harmonics suppression," *Progress In Electromagnetics Research Letters*, Vol. 17, 181–189, 2010.
9. Shum, K. M., Q. Xue, and C. H. Chan, "A novel microstrip ring hybrid incorporating a PBG cell," *IEEE Microw. Wireless Compon. Lett.*, Vol. 11, No. 6, 258–260, Jun. 2001.
10. Shie, C.-I., J.-C. Cheng, S.-C. Chou, and Y.-C. Chiang, "Design of cmos quadrature vco using on-chip trans-directional couplers," *Progress In Electromagnetics Research*, Vol. 106, 91–106, 2010.
11. Andrews, D. P. and C. S. Aitchison, "Wide-band lumped-element quadrature 3-dB couplers in microstrip," *IEEE Trans. Microw. Theory Tech.*, Vol. 48, No. 12, 2424–2431, Dec. 2000.
12. Sun, S. and L. Zhu, "Multiple-resonator-based bandpass filters," *IEEE Microwave Magazine*, Vol. 10, No. 2, 88–98, Apr. 2009.
13. Wu, Y.-L., C. Liao, and X.-Z. Xiong, "A dual-wideband bandpass filter based on e-shaped microstrip SIR with improved upper-stopband performance," *Progress In Electromagnetics Research*, Vol. 108, 141–153, 2010.
14. Wu, H.-W., S.-K. Liu, M.-H. Weng, and C.-H. Hung, "Compact microstrip bandpass filter with multispurious suppression," *Progress In Electromagnetics Research*, Vol. 107, 21–30, 2010.
15. Dai, G. and M. Xia, "Novel miniaturized bandpass filters using spiral-shaped resonators and window feed structures," *Progress In Electromagnetics Research*, Vol. 100, 235–243, 2010.
16. Yang, T., M. Tamura, and T. Itoh, "Compact hybrid resonator with series and shunt resonances used in miniaturized filters and balun filters," *IEEE Trans. Microw. Theory Tech.*, Vol. 58, No. 2, 390–402, Feb. 2010.
17. Yeung, L. K. and K.-L. Wu, "A dual-band coupled-line balun filter," *IEEE Trans. Microw. Theory Tech.*, Vol. 55, No. 11, 2406–2411, Nov. 2007.
18. Zheng, S. Y., W. S. Chan, and K. F. Man, "Multi-function patch element," *Progress In Electromagnetics Research*, Vol. 109, 159–174, 2010.
19. Yeung, L. K. and K.-L. Wu, "An integrated RF balanced-filter with enhanced rejection characteristics," *IEEE MTT-S Int. Microw. Symp. Dig.*, 713–716, 2005.
20. Yeung, L. K. and K.-L. Wu, "An LTCC balanced-to-unbalanced

extracted-pole bandpass filter with complex load," *IEEE Trans. Microw. Theory Tech.*, Vol. 54, No. 4, 1512–1518, Apr. 2006.

21. Watkins, J. and S. Uysal, "Novel microstrip directional band-pass/band-stop couplers and filters," *IEEE MTT-S Int. Microw. Symp. Dig.*, 411–414, 1990.
22. Uysal, S. and J. Watkins, "Novel microstrip multifunction directional couplers and filters for microwave and millimeter-wave applications," *IEEE Trans. Microw. Theory Tech.*, Vol. 39, No. 6, 977–985, Jun. 1991.
23. Chen, D. and C.-H. Cheng, "A novel compact ultra-wideband (UWB) wide slot antenna with via holes," *Progress In Electromagnetics Research*, Vol. 94, 343–349, 2009.
24. Kim, H., B. Lee, and M.-J. Park, "Dual-band branch-line coupler with port extensions," *IEEE Trans. Microw. Theory Tech.*, Vol. 58, No. 3, 651–655, Mar. 2010.
25. Park, M.-J., "Dual-band wilkinson divider with coupled output port extensions," *IEEE Trans. Microw. Theory Tech.*, Vol. 57, No. 9, 2232–2237, Sep. 2009.
26. Kawai, T., H. Taniguchi, I. Ohta, and A. Enokihara, "Broadband branch-line coupler with arbitrary power split ratio utilizing mircrostrip series stubs," *Proc. 40th Microw. Conf.*, 1170–1173, Sep. 2010.
27. Ashforth, J. V., "Design equations to realize a broadband hybrid ring or a two-branch guide coupler of any coupling coefficient," *Electron. Lett.*, Vol. 24, No. 20, 1276–1277, Sep. 1988.
28. Johnson, A. K. and G. I. Zysman, "Coupled transmission line networks in an inhomogeneous dielectric medium," *IEEE Trans. Microw. Theory Tech.*, Vol. 17, No. 10, 753–759, Oct. 1969.
29. Tripathi, V. K., "Asymmetric coupled transmission lines in an inhomogeneous medium," *IEEE Trans. Microw. Theory Tech.*, Vol. 23, No. 9, 734–739, Sep. 1975.